



Pyrrolobenzodiazepines (PBDs) Do Not Bind to DNA G-Quadruplexes

Khondaker M. Rahman*, David B. Corcoran, Tam T. T. Bui, Paul J. M. Jackson, David E. Thurston*

Department of Pharmacy, Institute of Pharmaceutical Science, King's College London, London, United Kingdom

Abstract

The pyrrolo[2,1-*c*][1,4] benzodiazepines (PBDs) are a family of sequence-selective, minor-groove binding DNA-interactive agents that covalently attach to guanine residues. A recent publication in *this journal* (Raju *et al*, *PLoS One*, 2012, 7, 4, e35920) reported that two PBD molecules were observed to bind with high affinity to the telomeric quadruplex of *Tetrahymena glaucoma* based on Electrospray Ionisation Mass Spectrometry (ESI-MS), Circular Dichroism, UV-Visible and Fluorescence spectroscopy data. This was a surprising result given the close 3-dimensional shape match between the structure of all PBD molecules and the minor groove of duplex DNA, and the completely different 3-dimensional structure of quadruplex DNA. Therefore, we evaluated the interaction of eight PBD molecules of diverse structure with a range of parallel, antiparallel and mixed DNA quadruplexes using DNA Thermal Denaturation, Circular Dichroism and Molecular Dynamics Simulations. Those PBD molecules without large C8-substituents had an insignificant affinity for the eight quadruplex types, although those with large π -system-containing C8-substituents (as with the compounds evaluated by Raju and co-workers) were found to interact to some extent. Our molecular dynamics simulations support the likelihood that molecules of this type, including those examined by Raju and co-workers, interact with quadruplex DNA through their C8-substituents rather than the PBD moiety itself. It is important for the literature to be clear on this matter, as the mechanism of action of these agents will be under close scrutiny in the near future due to the growing number of PBD-based agents entering the clinic as both single-agents and as components of antibody-drug conjugates (ADCs).

Citation: Rahman KM, Corcoran DB, Bui TTT, Jackson PJM, Thurston DE (2014) Pyrrolobenzodiazepines (PBDs) Do Not Bind to DNA G-Quadruplexes. *PLoS ONE* 9(8): e105021. doi:10.1371/journal.pone.0105021

Editor: Heidar-Ali Tajmir-Riahi, University of Quebec at Trois-Rivieres, Canada

Received: March 4, 2014; **Accepted:** July 15, 2014; **Published:** August 18, 2014

Copyright: © 2014 Rahman et al. This is an open-access article distributed under the terms of the Creative Commons Attribution License, which permits unrestricted use, distribution, and reproduction in any medium, provided the original author and source are credited.

Data Availability: The authors confirm that all data underlying the findings are fully available without restriction. All data are included within the paper.

Funding: This research was supported by internal funding available within King's College London. The funders had no role in study design, data collection and analysis, decision to publish, or preparation of the manuscript.

Competing Interests: The authors have declared that no competing interests exist.

* Email: k.miraz.rahman@kcl.ac.uk (KMR); david.thurston@kcl.ac.uk (DET)

Introduction

The pyrrolo[2,1-*c*][1,4] benzodiazepines (PBDs) are a group of sequence-selective DNA minor-groove binding agents originally discovered in *Streptomyces* species [1,2,3,4,5]. Anthramycin (**1**, **Figure 1**) was the first PBD to be isolated and studied [6], although more than twelve naturally occurring PBDs are now known [1]. They are characterized by an electrophilic N10–C11 imine group (or the hydrated equivalent) which forms a reversible covalent aminal linkage from their C11-position to the C2-NH₂ group of a guanine in the DNA minor groove [7,8]. Crucially, the molecules have (*S*)-chirality at their C11a-position, and this provides them with the appropriate 3-dimensional shape (*i.e.*, isohelicity) to fit perfectly into the DNA minor groove. PBD/DNA adduct formation has been shown to inhibit a number of biological processes, including the binding of transcription factors to DNA [9,10,11,12] and the function of enzymes such as endonucleases [13,14] and RNA polymerase [15]. Many PBD molecules also have significant antimicrobial activity [16,17,18,19,20,21].

PBD monomers have been shown by footprinting [7], NMR [22,23], molecular modeling [24] and X-ray crystallography [25] to span three base pairs with a reported preference for orientation of their A-ring toward the 3'-end of the covalently-modified strand (*i.e.*, A-Ring-3') [26], although a recent report suggests that the A-ring can orientate toward either the 3'- or 5'-ends [27]. In the

past, PBD molecules have been reported to prefer 5'-Pu-G-Pu-3' sequences [26,28], although more recent data suggest that they have a kinetic preference for 5'-Py-G-Py-3' motifs [27] (where Pu = purine, Py = pyrimidine, G = reacting guanine). PBDs are thought to interact with DNA by first locating a low-energy binding site through van der Waals (vdW), H-bonding and electrostatic interactions [29]. Once in place, nucleophilic attack by the exocyclic C2-NH₂ of the central guanine then occurs to form a covalent adduct [29]. Once bound, the PBD remains anchored in the DNA host minor groove, avoiding DNA repair through negligible distortion of the helix [25]. It is well-established that PBDs are highly selective in requiring minor groove structure in either duplex or hairpin DNA for covalent binding to occur, and they do not bind to single stranded DNA (or RNA) regardless of its GC content and/or length [30].

Synthetic PBD monomers with non-covalent DNA-interactive components joined to the C8-position of their A-rings have also been reported [29,31,32,33,34], and examples such as GWL-78 (**4**, **Figure 1**) [29] and KMR-28-18 (**5**, **Figure 1**) [12] can span up to six or seven base pairs. Furthermore, two PBD units have been joined through their C7- [35] or C8-positions (*i.e.*, **6-8**, **Figure 1**) to form PBD dimers with the ability to form inter- and intra-strand DNA cross-links [36,37]. One example (SJG-136, **6**) [38] is presently in Phase II clinical trials as an anti-cancer agent

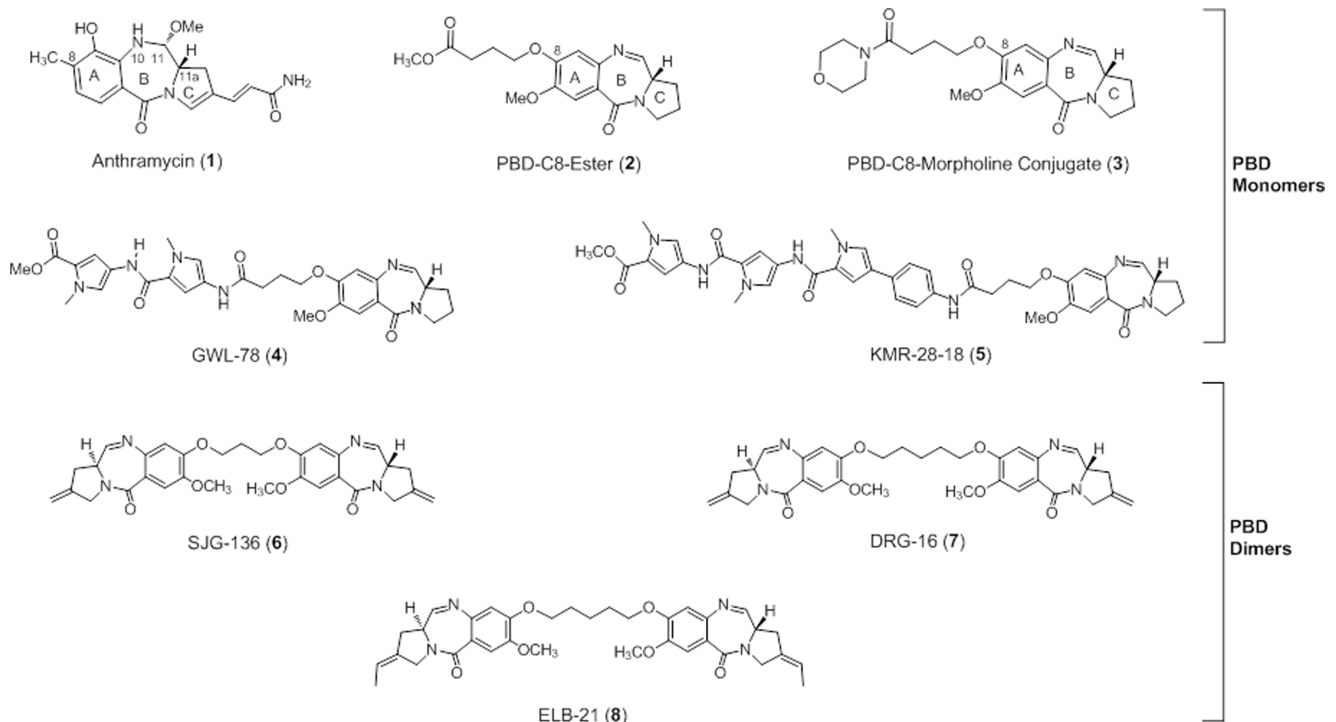


Figure 1. Structures of the PBD monomers and dimers used in the current study. Anthramycin methyl ether (1), the PBD-C8-ester (2) and the PBD-C8-morpholine (3) do not possess any π -systems in their C8-side chains, whereas the PBD C8-conjugates 4 and 5 both have C8-substituents consisting of aromatic rings. The three PBD dimers, SJG-136 (6), DRG-16 (7) and ELB-21 (8) have structural similarity to the PBD dimer (PBD2, 10) evaluated by Raju and co-workers [53] (see Figure 2). doi:10.1371/journal.pone.0105021.g001

[39,40,41]. Both PBD monomers and dimers have a common feature in that their covalent interaction in the minor groove significantly enhances the stability of the DNA double helix to thermal denaturation [26,29,42], and this stabilizing property correlates well with their *in vitro* cytotoxicity [29,38,42].

Although B-Form DNA is the predominant type present in cells, it is now known that single-stranded guanine-rich nucleic acid sequences can fold into four-stranded structures comprised of stacked tetrads formed by Hoogsteen hydrogen bonding of four guanines, stabilized overall by monovalent cations such as K^+ . These structures, known as G-quadruplexes (or G4s), are classified by their sequence, stoichiometry, polarity of each strand, how the loops connect the different strands, and the conformation of guanine glycosidic angles. For example, G-quadruplexes can be classified as uni-, bi- or tetra-molecular, and can have differences in loop directionality (*e.g.*, parallel or antiparallel) and length. Certain proteins known as telomere end-binding proteins (TEBPs) can promote G-quadruplex formation under the control of the cell cycle machinery [43].

G-quadruplexes may form in telomeric DNA repeats as well as in sequences in the promoter and other regulatory regions within human and other genomes. The human genome has been surveyed for putative G4-forming sequences, and over 250,000 non-overlapping sequences have been identified [43], with many over-represented in promoter regions and in the first intron [44] of a variety of genes. Putative G4-forming regions of DNA have at least four runs of three or more consecutive guanines (G-tracts) separated by varying nucleotides that comprise the loop structures. Negative superhelicity induced by transcription can promote local unwinding of these G/C-rich duplex regions of DNA, allowing for the formation of G4s. Interestingly, a correlation has been found

between the frequency of occurrence of these sequences in promoter regions and the nuclease hypersensitivity of these sites. Even though G4 formation has to compete with the stable duplex DNA form, a number of studies have shown that G4 structures can be induced under conditions which mimic the intracellular environment, and that they can have significant biological consequences [45,46]. Crucially, G4s have recently been shown to form in cells, and to play a role in modulating transcription [47,48,49]. Their unique, non-B-form globular structure, and their potential to regulate the transcription of a range of oncogenes, have made G4s an attractive target for the development of novel anticancer agents. For example, a number of genes involved in the proliferation of tumour cells such as *C-myc*, *c-Kit*, *BCL2* and *K-ras* are known to contain G4-forming sequences in their promoter regions [50] and are being targeted. In a number of these, stable G4 structures have been demonstrated to form using biophysical methods, and in others (*e.g.*, *C-myc*, *c-Kit*, *K-ras*, *PDGFA* and *BCL2*) [51,52] the molecular structures of promoter quadruplexes have been characterized by high-field NMR.

Despite the fact that it is well-established that G-quadruplexes do not possess any B-form duplex DNA structure or minor groove environment, and that it is known that small molecules can discriminate between DNA duplex and quadruplex architectures [50], Raju and co-workers recently reported [53] that two DNA minor-groove binding PBD molecules, the C8-linked PBD-pyrene conjugate (9, Figure 2) and the mixed N10-C11/N10'-C11' imine-lactam pyrrolobenzodiazepine dimer (10, Figure 2) bind with high affinity to the G-quadruplex formed in a telomeric region of DNA from *Tetrahymena* Glaucoma. This was surprising given the extensive literature on PBD agents since the 1960s, all of which highlight the close 3-dimensional fit of these molecules in

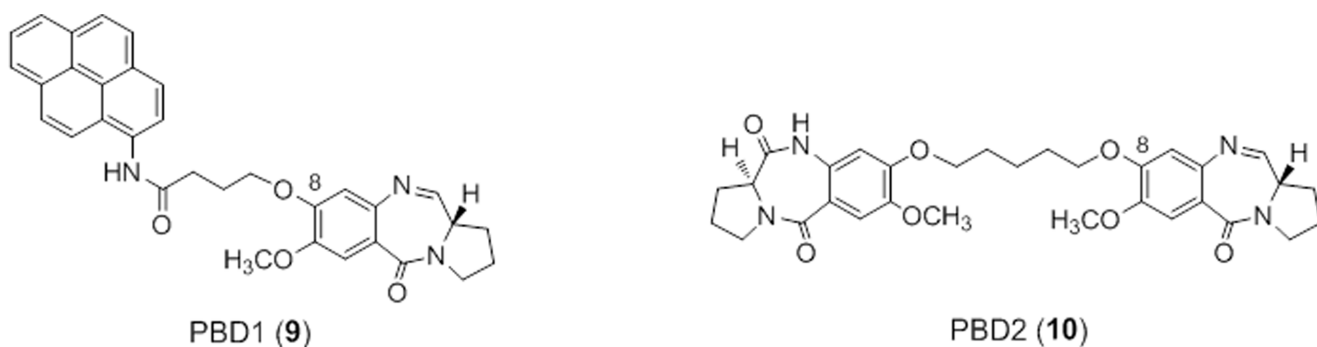


Figure 2. Structures of the C8-substituted PBD-Pyrene conjugate (PBD1, 9) and the PBD dimer (PBD2, 10) reported by Raju and co-workers to bind to quadruplex DNA [53].
doi:10.1371/journal.pone.0105021.g002

the minor groove of B-Form DNA [26,28]. It is also known that PBDs do not bind to RNA due to the lack of a minor groove environment in this type of nucleic acid structure [54]. In addition, we have previously used PBD molecules as negative controls in screens searching for quadruplex-binding ligands (*un-reported results*).

This prompted us to carry out a detailed evaluation of the potential interaction of eight pyrrolobenzodiazepine molecules of both monomer (**1–5**) and dimer (**6–8**) types of diverse structure (**Figure 1**) with eight different G-quadruplex-forming sequences including the same *Tetrahymena* glaucoma sequence used by Raju and co-workers [53] (**Table 1**). To evaluate quadruplex *versus* duplex binding, we initially utilised a well-established FRET-based melting assay [55,56], along with a control biaryl polyamide molecule KMR-04-12 (**11**, **Figure 3**), previously reported [55] to be highly selective for quadruplex *versus* duplex DNA. Despite evaluating the eight pyrrolobenzodiazepine compounds up to very high concentrations (*i.e.*, 5:1 to 50:1 ligand/DNA molar ratios), six did not show any significant stabilisation of any of the eight G-quadruplex structures, whereas GWL-78 (**4**) and KMR-28-18 (**5**) had modest stabilizing properties (*i.e.*, up to $\Delta T_m = 2.9^\circ\text{C}$) at the highest concentration tested (*i.e.*, 50 μM , 50:1 ligand/DNA molar ratio). This compared to a ΔT_m value of up to 25.1°C for the positive quadruplex-binding control molecule **11** at the same concentration and molar ratio. Conversely, when the PBDs were evaluated against duplex DNA at the same concentration and molar ratio, ΔT_m values ranged from 4.5°C for the simple PBD C8-Ester (**2**) to 28°C for the PBD dimer SJG-136 (**6**), whereas the quadruplex-binding control molecule **11** had a ΔT_m of only 1.1°C at the same concentration and molar ratio.

It is noteworthy that **4** and **5** have the longest C8-substituents of all the PBDs evaluated. Significantly, the isolated PBD core unit

alone with the short C8-substituent (**2**, **Figure 1**) had no stabilising properties toward quadruplex DNA, confirming that it was the MPB-Py-Py C8-substituent itself rather than the PBD component providing the quadruplex binding properties. To investigate this further, the isolated MPB-Py-Py fragment (**12**, **Figure 3**) that comprises the C8-substituent of **5** was evaluated and found to have a ΔT_m value of up to 2.9°C at a 50:1 ligand/DNA molar ratio. In the case of the PBD1 (**9**) and PBD2 (**10**) molecules studied by Raju and co-workers [53], it is likely that a similar phenomenon was taking place during their experiments, with the relatively bulky C8-substituents binding to the quadruplex DNA rather than the PBD components. In our study, the relative lack of interaction of the eight PBD molecules with the different quadruplex sequences was further confirmed by CD spectroscopy which failed to show any notable change in the characteristic signals after the addition of up to 10 molar equivalents of ligands. Molecular modeling studies also supported these observations.

Materials and Methods

Fluorescence Resonance Energy Transfer (FRET) Assay

Oligonucleotide sequences used for the FRET-based DNA thermal denaturation assays (see **Table 1**) were purchased from Eurogentec, Southampton, UK. TAMRA (6-carboxytetramethylrhodamine) and FAM (6-carboxyfluorescein) are acceptor and donor fluorophores, respectively. From 20 μM stock solutions, 400 nM solutions in FRET buffer (optimized as 50 mM potassium, 50 mM cacodylate, pH 7.4) were prepared prior to use. The oligonucleotides were annealed through heating the samples to 90°C for 10 mins followed by cooling to room temperature and storing at this temperature for 5 h. Dilutions from the initial 5 mM DMSO stock solution were performed using FRET buffer.

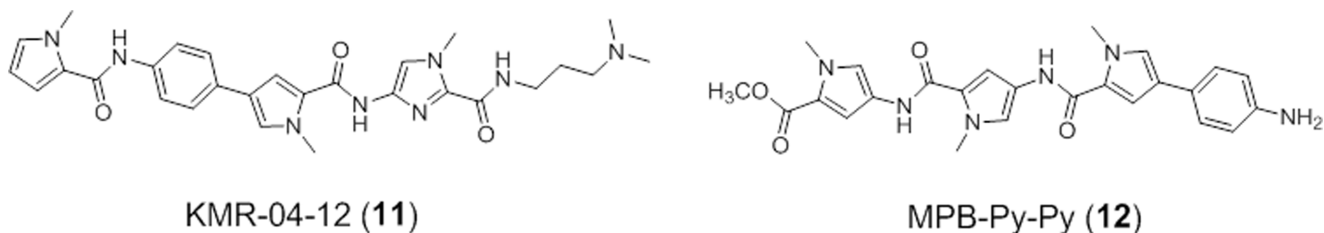


Figure 3. Structures of the G-quadruplex-interacting ligand KMR-04-12 (11), and the MPB-Py-Py fragment (12) identical to the C8-side chain of KMR-28-18 (5). The MPB moiety in the centre of KMR-04-12 (11) provides the molecule with a U-shaped 3-dimensional shape suitable for binding to G-quadruplex DNA.
doi:10.1371/journal.pone.0105021.g003

Table 1. G-Quadruplex-forming oligonucleotides used in this study.

Source Gene	Topology in K ⁺ Buffer ^a	Base Pair Sequence
<i>F21T</i>	M	5'-FAM-GGGTTAGGGTTAGGGTTAGGG-TAMRA-3'
<i>FT2G8</i>	P	5'-FAM-GGGGTTGGGG-TAMRA-3'
<i>c-Kit1</i>	A	5'-FAM-d(G ₃ AG ₃ CGCTG ₃ AG ₂ AG ₃)-TAMRA-3'
<i>c-Kit2</i>	A	5'-FAM-d(G ₃ CG ₃ CGCGAG ₃ AG ₄)-TAMRA-3'
<i>C-myc</i>	P	5'-FAM-TGGGGAGGGTGGGGAGGGTGGGGAAGG-TAMRA-3'
<i>K-ras</i>	P	5'-FAM-GGGAGGGAGGGAAGGAGGGAGGGAGGGA-TAMRA-3'
<i>STAT3</i>	P	5'-FAM-GGGCTGGGGATGGGGAGGGGG-TAMRA-3'
<i>BCL2</i>	P	5'-FAM-GGGCGCGGAGGGAAGGGGCGGG-TAMRA-3'
Duplex		5'-FAM-(TA) ₂ GC(TA) ₂ AGAT ₆ TCT(TA) ₂ GC(TA) ₂ -TAMRA-3'

^aM = Mixed Parallel/Anti-Parallel; P = Parallel; A = Anti-Parallel.

doi:10.1371/journal.pone.0105021.t001

Annealed DNA (25 μ L) and sample solution (25 μ L) were added to each well of a 96-well plate (MJ Research, Waltham, MA), and processed in a DNA Engine Opticon (MJ Research). Fluorescence readings were taken at intervals of 0.5°C over the range 30–100°C, with a constant temperature maintained for 30 seconds prior to each reading. Incident radiation of 450–495 nm was used, with detection at 515–545 nm. The raw data were imported into the program Origin (Version 7.0, OringinLab Corp.), and the graphs were smoothed using a 10-point running average, and then normalized. Determination of melting temperatures was based on values at the maxima of the first derivative of the smoothed melting curves using a script. The difference between the melting temperature of each sample and that of the blank (ΔT_m) was used for comparative purposes.

Circular Dichroism and Thermal Denaturation Studies

The UV & CD spectra of the oligonucleotides and oligonucleotide/ligand complexes were acquired using a Chirascan-Plus Spectrometer (Applied Photophysics Ltd, Leatherhead, UK). The UV absorbance and CD spectra were measured between 500–200 nm in a strain-free rectangular 5 or 10 mm cell. The instrument was flushed continuously with pure evaporated nitrogen throughout the measurements. Spectra were recorded using a 1 nm step size, a 1 s time-per-point and a spectral bandwidth of 1 or 2 nm. Addition of the ligands to the oligonucleotide solutions was carried out while maintaining a constant concentration of DNA. All spectra were acquired at room temperature and the buffer baseline corrected. All CD spectra were smoothed using the Savitsky-Golay method, and a window factor of 4–12 was used for better presentation.

The Dynamic Multi-mode Spectroscopy (DMS) technology provided by Applied Photophysics Ltd was employed for the thermal measurements. The CD spectra were first recorded at room temperature (20°C), then after cooling to 6°C, heating to the highest temperature (94°C), re-cooling to 6°C and finally heating back to 20°C. The melting profiles monitored at a particular wavelength were recorded during both the heating and cooling processes. The instrument was equipped with a Quantum (NorthWest, USA) TC125 Peltier unit set to change temperature from 6→94°C at a rate of 1°C/min with a 2°C step-size. The same parameters were set for the cooling process (94→6°C). A 2 s time-per-points CD measurement time scale was employed in the 400–215 nm region with a 2 nm spectral bandwidth. Temperature was measured directly using a thermocouple probe in the solutions. Melting temperatures were determined from derivative

spectra produced using the Global Analysis T-Ramp software (Applied Photophysics Ltd).

Molecular Modeling Studies

All MD simulations were performed using the AMBER 11 software package [57].

Ligand Preparation. The PBD structures KMR-28-18 (**5**), DRG-16 (**7**), PBD1 (**9**) and PBD2 (**10**) were constructed using the Schrödinger Maestro software, and the dihedrals of each structure were rotated to maintain the known curved nature (“isohelicity”) of the PBD molecules. AMBER *antechamber* was used to assign partial atomic charges to each ligand using the Gasteiger charging system, and missing parameters were generated for each ligand using AMBER *parmchk*. Ligands were then energy minimized using the MMFF94 energy gradient.

Receptor Preparation. Structural co-ordinates of the G-quadruplex receptor file were obtained from the Protein Data Bank (PDB ID: 3CDM) [58]. The coordinates were subjected to molecular mechanics minimization (1000 steps steepest descent, followed by 3000 steps of Polak-Ribiere conjugate gradient minimization with a derivative convergence of 0.05 kJ \AA^{-1} mol), followed by molecular dynamics simulation (40 ps at 300 K equilibrium using a 1.5 fs time-step). A final molecular mechanics minimization (Polak-Ribiere conjugate gradient) of the average co-ordinates of the previous MD step was then undertaken to obtain a final model of low energy for use in ligand:DNA studies [59].

DNA-Drug Adduct Simulation. AMBER *xleap* was used to align each ligand with the outer face of the quadruplex structure, with initial coordinate and topology files established using ff99bsc0 force field parameters [60] (for DNA) and *gaff* parameters for each ligand. AMBER *xleap* was used to automatically place 21 K⁺ counter-ions around the quadruplex structure, and a 12 \AA truncated octahedral periodic water solvent box (TIP3P) and periodic boundary conditions were created for use in simulations. Initial energy minimization was undertaken with DNA restrained at a high force constant (500 kcal mol⁻¹ \AA^{-2}), which was reduced in stages to zero. In the first stage of MD simulation, a 30 ps simulation was performed where the system was heated slowly from 0 K to 300 K using the Langevin thermostat (and a collision frequency of 1.0 ps⁻¹). Following this, an equilibration step was undertaken over 100 ps with constant pressure and no restraints. Production dynamics simulations were then run over a time-scale of 10 ns (constant volume, 300 K temperature) with a 2 fs time step. The SHAKE algorithm was applied to restrain hydrogen atoms, thereby removing the highest frequency oscillation and

Table 2. FRET-based DNA thermal denaturation assay results (ΔT_m values) for the interaction of the PBD monomers (1–5) and dimers (6–8) (Figure 1) with eight different G-quadruplex-forming DNA sequences and a duplex DNA control (Table 1).

Ligand	Ligand Conc. (μ M) (Ligand:G4)	ΔT_m [$^{\circ}$ C] ^a									
		F217	FT2G8	c-Kit1	c-Kit2	C-myc	K-ras	STAT3	BCL2	Duplex	
Anthracyclin (1)	50 (50:1) ^b	0	0	0	0	0	0	0	0	0	18
	10 (50:1)	0	0	0	0	0	0	0	0	0	14
	5 (25:1)	0	0	0	0	0	0	0	0	0	12
PBD-C8-Ester (2)	1 (5:1)	0	0	0	0	0	0	0	0	0	11
	50 (50:1) ^b	0	0	0	0	0	0	0	0	0	4.7
	10 (50:1)	0	0	0	0	0	0	0	0	0	4.5
PBD-C8-Morpholine (3)	5 (25:1)	0	0	0	0	0	0	0	0	0	4.0
	1 (5:1)	0	0	0	0	0	0	0	0	0	2.3
	50 (50:1) ^b	0	0	0	0	0	0	0	0	0	7.1
GWL-78 (4)	10 (50:1)	0	0	0	0	0	0	0	0	0	6.6
	5 (25:1)	0	0	0	0	0	0	0	0	0	7.5
	1 (5:1)	0	0	0	0	0	0	0	0	0	6
KMR-28-18 (5)	50 (50:1) ^b	1.5	1.5	2.2	2.0	0	2.3	2.0	2.0	2.0	23
	10 (50:1)	1.2	1.2	2.0	2.1	0	2.1	1.8	1.9	1.9	24
	5 (25:1)	1.1	0.6	1.2	1.4	0	1.1	1.1	0.8	0.8	19
SJM-136 (6)	1 (5:1)	0	0	0	0	0	0	0	0	0	17
	50 (50:1) ^b	2.5	2.0	2.3	2.7	1	2.2	2.0	2.1	2.1	18
	10 (50:1)	2.8	2.1	2.5	2.9	1	2.4	2.2	2.4	2.4	20
DRG-16 (7)	5 (25:1)	1.0	1.2	2.2	2.4	0.5	2.1	2.0	1.8	1.8	18
	1 (5:1)	0.5	0.5	0.5	0.5	0	0.5	0	0.5	0.5	14
	50 (50:1) ^b	0.9	0.0	0.6	0.8	0	1.4	1.1	0.8	0.8	23
ELB-21 (8)	10 (50:1)	0.8	0.0	0.8	1.0	0	1.1	1.2	0.8	0.8	28
	5 (25:1)	0.6	0.5	0.7	0.7	0	0.8	0.7	0.5	0.5	22
	1 (5:1)	0	0	0	0	0	0	0	0	0	17
KMR-04-12 (11)	10 (50:1)	1.0	0.7	0.9	0.8	0	1.5	1.7	1.1	1.1	28
	5 (25:1)	0.8	0.5	0.6	0.6	0	0.8	0.6	0.8	0.8	21
	1 (5:1)	0	0	0	0	0	0	0	0	0	18
KMR-04-12 (11)	50 (50:1) ^b	0.8	0.7	0.6	0.8	0	0.8	0.9	0.8	0.8	25
	5 (25:1)	0.6	0.6	0.5	0.6	0	0.6	0.5	0.8	0.8	24
	1 (5:1)	0	0	0	0	0	0	0	0	0	17
KMR-04-12 (11)	50 (50:1) ^b	26.5	18.5	15.3	14.5	5.5	14.2	12.5	12.0	12.0	1.5
	10 (50:1)	25.1	17.1	14.5	15.6	4.5	13.7	11.2	12.3	12.3	1.1
	5 (25:1)	17.5	12.5	10.6	8.5	2.3	11.3	8.6	10.5	10.5	0.7

Table 2. Cont.

Ligand	Ligand Conc. [μM] (Ligand:G4)	ΔT_m [$^{\circ}\text{C}$] ^a								
		F217	FT2G8	c-Kit1	c-Kit2	C-myc	K-ras	STAT3	BCL2	Duplex
1 (5:1)		8.8	4.6	6.1	3.2	2.1	7.7	5.7	6.2	0
MPB-Py-Py (12)	50 (50:1) ^b	2.0	2.1	2.0	2.2	0	2.1	2.2	1.8	1.4
	10 (50:1)	1.8	1.6	1.9	2.1	0	1.1	1.8	1.9	1.2
	5 (25:1)	0.8	1.1	1.5	1.6	0	1.5	1.6	1.8	1.0
	1 (5:1)	0	0.5	0	0.5	0	0.5	0	0.5	0

KMR-04-12 (11, Figure 3) was included as a positive quadruplex-binding control molecule, and the MPB-Py-Py fragment 12 (Figure 3) was evaluated to represent the isolated C8-substituent of the PBD C8-Conjugate 5 (Figure 1).

^aESDS $\pm 0.5^{\circ}\text{C}$
^bConcentration of DNA was 1 μM in these experiments; in all other cases it was 200 nM. Differences in ΔT_m values for duplex DNA at the highest ligand concentration of 50 μM (50:1, ligand:G4) are thought to be due to solubility or aggregation issues at these artificially high concentrations of ligand and DNA.
 doi:10.1371/journal.pone.0105021.t002

permitting the use of a 2 fs time-step, with all simulations undertaken using AMBER *pmemd*. Molecular dynamics simulations were visualised using VMD [61], and models were created using Chimera [62].

Free Energy of Binding Calculations. Binding free energy was calculated using the following equation:

$$\Delta G_{bind}^{\circ} = \Delta G_{bind\ vacuum}^{\circ} + \Delta G_{complex}^{\circ} - (\Delta G_{ligand}^{\circ} + \Delta G_{receptor}^{\circ}),$$

where ΔG_{bind}° was determined by solving the linearized Poisson-Boltzmann equation [63]:

$$\Delta G_{complex}^{\circ} = E_{MM} + G_{polar\ solvation\ energy} + G_{nonpolar\ solvation\ energy} - TS$$

Solvation energies (both polar and non-polar) were considered, with E_{MM} corresponding to internal, electrostatic and van der Waal interactions, and S to solute entropy.

The final binding energy was represented using the equation:

$$\Delta G_{bind}^{\circ} = \Delta E_{MM} + \Delta G_{solv}^{\circ} - T\Delta S$$

Entropic calculations were not undertaken as they are computationally expensive and are prone to introducing significant errors into the calculation of free energy of binding values. Furthermore, due to the fact that similar entropic states (*i.e.*, identical receptors and structurally similar ligands) were analyzed, computationally expensive entropic calculations would have added little value to the free energy of binding results. One hundred snapshots of the MD simulations were taken at equal intervals over the 10 ns duration, and molecular mechanics (MM) calculations were performed using *pbsa* [64].

Results and Discussion

The initial experiments involved measurement of the interaction of PBDs 1–8 (Figure 1) and the quadruplex-binding control molecule 11 (Figure 3) with the eight quadruplex-forming DNA sequences and the control DNA duplex shown in Table 1 using the Fluorescence Resonance Energy Transfer (FRET) thermal denaturation assay described in the *Materials and Methods* section. FRET assays are widely used to determine melting temperatures of different DNA sequences and ligand-DNA complexes [65,66], and the FRET phenomenon has been extensively used to study the stability of nucleic acid structures and, in particular, G-quadruplex DNA [65]. In the FRET-based G-quadruplex melting assay used in this study, 6-carboxyfluorescein (FAM) and 6-carboxytetramethylrhodamine (TAMRA) were used as donor and acceptor FRET moieties attached to the 5'- and 3'- ends of the DNA, respectively, via 6-carbon linkers [66]. The FAM/TAMRA fluorophore pair has a Forster radius (R_0) of approximately 5 nm, and when the labeled sequences form G-quadruplexes, the two are located close enough to allow FRET to occur efficiently. Application of external energy in the form of heat unfolds the quadruplex causing the fluorophores to separate from each other, thus reducing the FRET efficiency and generating a signal through a consequent increase in the intensity of radiation emitted by the donor.

The results (Table 2) confirm that the PBD monomers without heterocycle-containing C8-substituents (1–3), all failed to stabilise the eight G-quadruplex sequences even at a molar ratio of 50:1 (Ligand:G-quadruplex - 10 μM :0.2 μM and 50 μM :1 μM). This

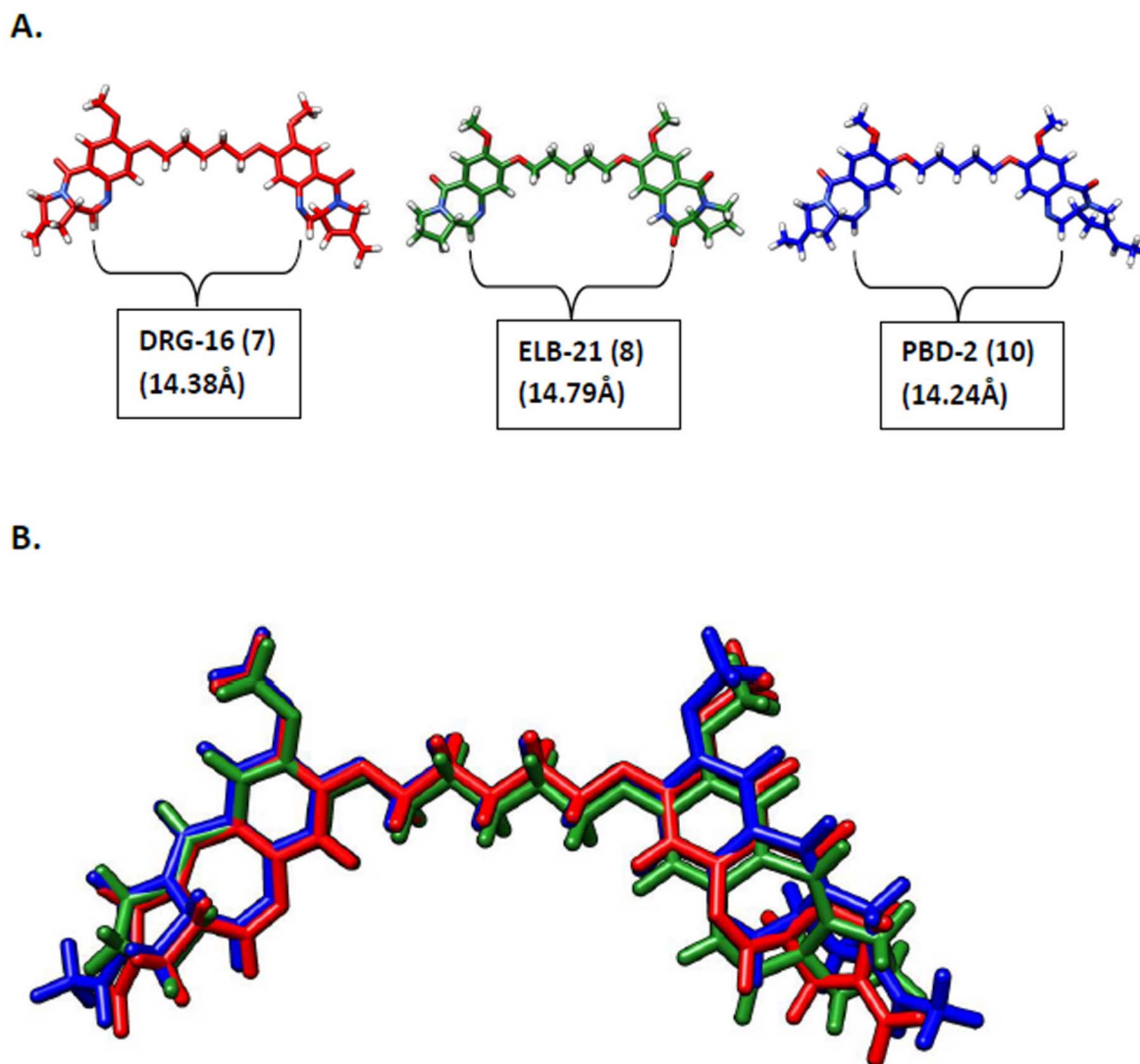


Figure 4. A, Comparison of length and 3-dimensional shape between the PBD dimer (PBD2, **10**) used in the G-quadruplex studies reported by Raju and co-workers [53] and the PBD dimers **7** and **8** used in this study; **B,** Overlay of the three PBD dimers (**7**, **8** and **10**) confirming their superimposability.

doi:10.1371/journal.pone.0105021.g004

was anticipated, as the molecules are not planar and contain no appreciable π -ring systems (apart from the PBD A-ring) that can interact with the quadruplex structure, a known means to enhance ligand/quadruplex affinity [67,68]. On the other hand, the PBD-C8 conjugates with π -ring-containing C8-substituents (**4** and **5**) showed negligible stabilisation at a molar ratio of ligand/quadruplex of up to 5:1, but a modest increase in melting temperatures (*i.e.*, up to 2.4°C) of almost all the G-quadruplexes at a 25:1 ratio (Ligand:G-quadruplex - 5 μ M:0.2 μ M), increasing marginally to up to 2.9°C at a 50:1 molar ratio (Ligand:G-quadruplex - 10 μ M:0.2 μ M and 50 μ M:1 μ M). This suggested that, for these molecules, the stabilisation was due to the heterocyclic rings attached to the C8-position, particularly as the shorter C8-substituent of **4** led to a lower enhancement in T_m than the longer side chain of **5**. To probe this further, we evaluated the dipyrrole-MPB moiety **12** (Figure 3), identical in structure to the C8-substituent of KMR-28-18 (**5**), at the same concentrations as used for the PBD-C8 conjugates. Interestingly, it produced an almost identical interaction profile, stabilising all of the different

G-quadruplex sequences by up to 2.1°C at a 50:1 molar ratio (Ligand:G-quadruplex - 10 μ M:0.2 μ M and 50 μ M:1 μ M). This result, coupled with the fact that the simple PBD monomers **1–3** had no quadruplex stabilising activity of their own even at the highest concentration and molar ratio, confirmed that PBD structures themselves are not capable of stabilizing DNA quadruplex.

Next, we studied the PBD dimers **6–8** for their ability to interact with and stabilise the G-quadruplex sequences. PBD dimers **7** and **8** are similar to the PBD2 (**10**) molecule (Figure 2) studied by Raju and co-workers in having a C8/C8'-dioxypentenyl linker joining the two A-rings of the PBD units. Although they contain N10-C11/N10'-C11' imine moieties rather than the mixed imine/dilactam functionalities present in PBD2 (**10**) at these positions, this does not affect their length or 3-dimensional shape (see Figure 4). However, no stabilisation was observed for any of the quadruplex-forming sequences at molar ratios of up to 10:1 (ligand:G-quadruplex). The shorter PBD dimer SJG-136 (**6**) that contains a C8/C8'-dioxypentenyl linker was similarly non-

Induced CD spectra, 10mm pathlength

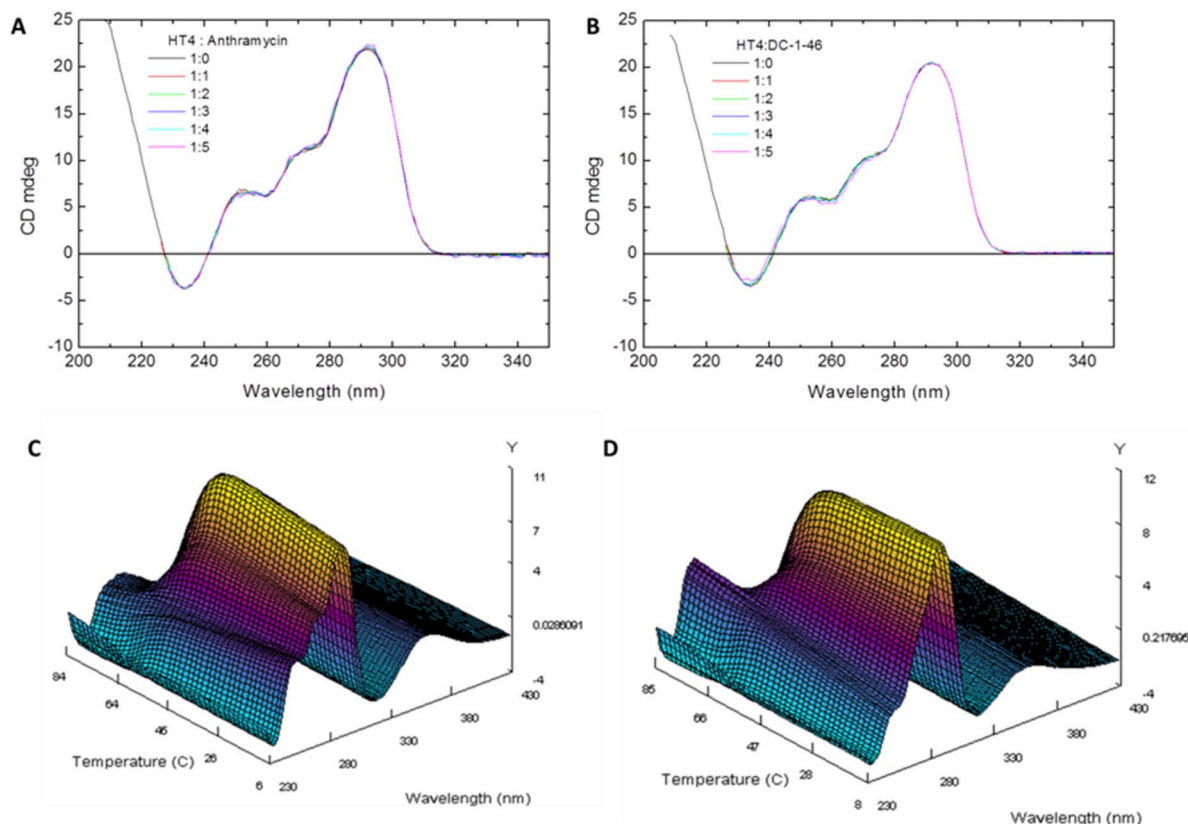


Figure 5. A & B, CD titration of anthramycin (**1**) and the C8-PBD-morpholine (**3**), respectively, with the telomeric G-quadruplex sequence (HT4) demonstrating a lack of interaction; **C & D**, CD melting profile of anthramycin:HT4 and C8-PBD-morpholine (**3**):HT4, respectively. For both molecules there was no change in CD melting temperature compared to the HT4 DNA alone.
doi:10.1371/journal.pone.0105021.g005

interactive. A modest increase in melting temperature was observed for all three PBD dimers (*i.e.*, up to 1.7°C) at the higher 50:1 ratio (Ligand:G-quadruplex - 10 μ M:0.2 μ M), most likely due to a non-selective interaction with the loop sequences where the dimers may be able to form hairpin-like structures around the DNA bases at such high concentrations.

To further confirm the lack of interaction of PBD monomers and dimers with G-quadruplex sequences, CD titration and CD melting studies were carried out with the PBD monomer anthramycin (**1**) and the C8-linked PBD-morpholine conjugate **3** with the human telomeric G-quadruplex sequence HT4. This quadruplex was selected as it is one of the most studied structures, and a number of CD titration experiments with G-quadruplex-binding ligands have been reported [45,51,56,67,69]. The CD spectrum of the HT4 sequence showed the characteristic presence of mixed parallel and antiparallel structures with positive peaks around 295 nm and a negative peak around 240 nm (**Figure 5**). Neither **1** or **3** produced any notable changes in the CD signals at the highest ratio evaluated (5:1; ligand:HT4). Furthermore, no change in melting temperatures in the presence or absence of the ligands was observed in the CD melting experiment. On the other hand, for the known quadruplex-binding ligand KMR-04-12 (**11**, **Figure 3**), we observed a concentration-dependent enhancement of the major positive peak at 295 nm, a concentration dependent appearance of a major negative peak around 260 nm, and a concentration dependent disappearance of the negative peak

around 240 nm, all confirming association of the ligand with the telomeric G-quadruplex structure (**Figure 6**).

Next, a detailed molecular modelling study was carried out to further confirm the lack of interaction of pyrrolobenzodiazepine dimers with G-quadruplex DNA. For this study we selected the PBD dimer PBD2 (**10**) reported by Raju and co-workers [53], and the two structurally similar PBD dimers **7** and **8**, both of which have been previously reported in the literature [1,21] and have similar length and 3-dimensional structure (**Figure 4A**). Furthermore, an overlay of **7**, **8** and **10** shows that each one occupies similar 3-dimensional space and should cover a near-identical span of DNA bases (**Figure 4B**). As the shape and curvature of each structure is identical, PBD2 (**10**) would be expected to interact with duplex rather than quadruplex DNA in a similar manner to **7** and **8**. Although we did not have access to PBD2 (**10**), the shape similarity between these three PBD dimers should enable extrapolation of the experimental results obtained to **10**. As we did not observe any notable stabilisation of the G-quadruplex sequences (including the *Tetrahymena* G-quadruplex) by either **7** or **8**, it would appear unlikely that PBD2 (**10**) could provide the strong G-quadruplex stabilisation reported by Raju and co-workers [53].

Finally, we carried out molecular dynamics studies on the C8-pyrene conjugate (PBD1, **9**, **Figure 2**) reported by Raju and co-workers, and the C8-MPB-Py-Py conjugate (**5**, **Figure 1**) used in our study, to elucidate a possible mechanism of binding of these

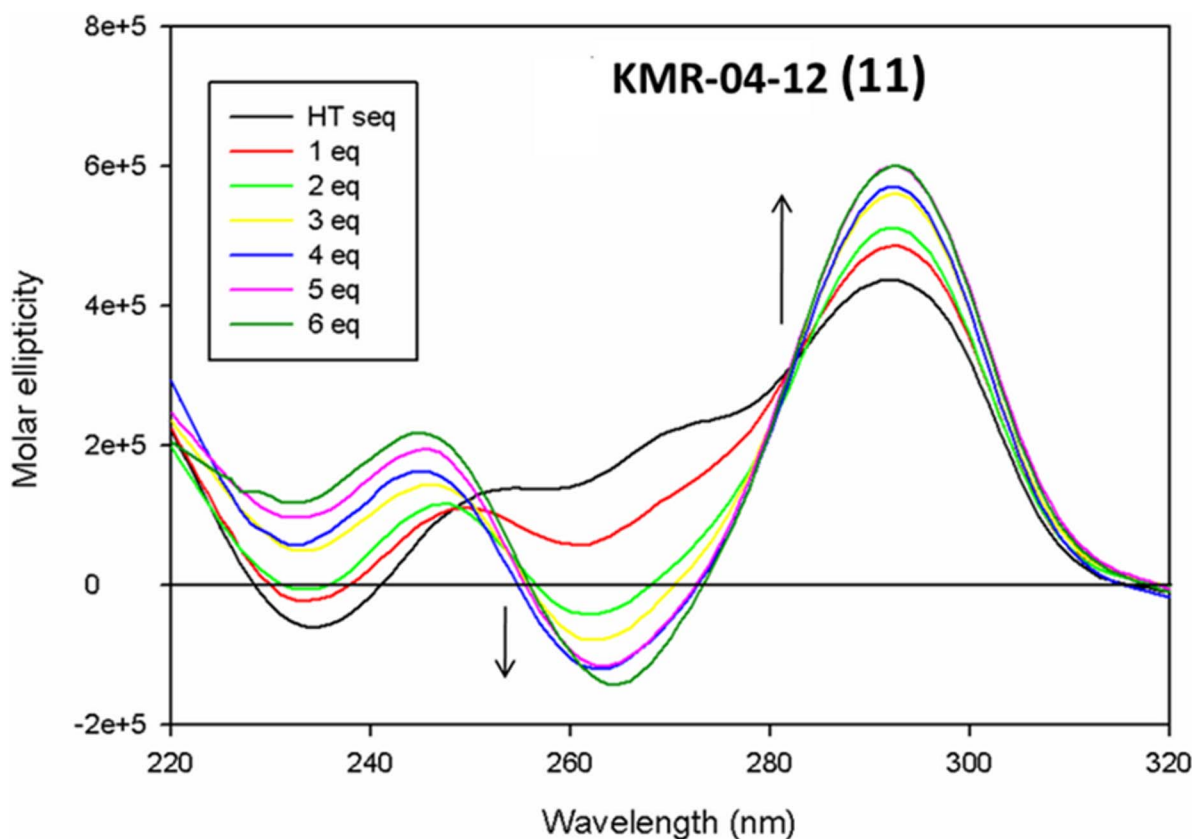


Figure 6. CD spectrum of a 5 μ M solution of telomeric G-quadruplex with 0–6 equivalents of KMR-04-12 (11), showing dose-dependent enhancement of the CD signals.

doi:10.1371/journal.pone.0105021.g006

molecules to quadruplex DNA. In the FRET-DNA melting study, **5** provided modest G-quadruplex stabilisation of up to 2.9°C at a molar ratio of 50:1 (ligand:DNA). The crystal structure of a telomeric G-quadruplex (PDB ID: 3CDM) was taken as a starting point to study plausible interactions with **5** and **9**. In both cases, the MD simulations suggested that quadruplex binding was mediated exclusively by the C8-linked components and not by the PBD ring structure itself. In the case of **9**, when it was placed over the G-quartet, the planar pyrene fragment appeared to be ideally shaped for interaction with the G-quadruplex structure. In the initial stages of the simulation, the pyrene moiety interacted in a non-covalent manner with the G-quadruplex sequence, with the pyrrolobenzodiazepine unit pointing upwards in an orthogonal position to the pyrene moiety (**Figure 7a**). As the simulation progressed, the PBD fragment was gradually pulled further towards the quadruplex structure, but did not participate in any significant interactions with the DNA. Further simulations were undertaken starting with the PBD placed over the G-quadruplex and the pyrene oriented at an angle orthogonal to the G quartet. However, in these simulations the PBD shifted away from the quadruplex structure and was replaced by the pyrene which then stabilised the G-quadruplex to a much greater extent. In the case of the PBD-MPB conjugate **5**, which exhibited moderate G-quadruplex stabilisation, simulations of the ligand interacting with the quadruplex produced similar results to those for the PBD-Pyrene (**9**), with the non-covalent moiety (*i.e.*, the C8-MPB-Py-Py fragment) interacting with the G-quadruplex structure while the PBD remained outside of the plane of the DNA. These observations were further supported by free energy of binding

calculations conducted during simulations of the interaction of the C8-Pyrene conjugate (**9**) with the G-quadruplex compared to similar calculations for interaction of the pyrene fragment alone with the quadruplex. These calculations gave a more favourable free energy of binding for the pyrene fragment alone (−19.50 kcal/mol) compared to the C8-Pyrene PBD conjugate (**9**) (−17.94 kcal/mol), suggesting that the presence of the PBD fragment may actually reduce DNA interactivity rather than enhance it. Taken together, these simulations and energy calculations unequivocally supported our view that it is the non-covalent C8-moieties of the ligands (*i.e.*, the MPB-Py-Py and pyrene fragments of **5** and **9**, respectively) that direct and facilitate quadruplex binding rather than the PBD entities themselves, which have no affinity for quadruplex DNA.

Conclusion

Despite the report by Raju and co-workers [53] that PBD molecules can stabilise quadruplex DNA structures, we can find no evidence to substantiate this claim based on FRET thermal denaturation, CD studies, molecular dynamics simulations and free energy of binding calculations of the potential interaction of eight PBD molecules of diverse structure with eight different DNA quadruplex types. For some PBD-containing molecules we did observe moderate binding at high molar ratios of ligand/DNA, but this only occurred to a significant extent for PBD molecules with large C8-substituents (*e.g.*, **4** and **5**). We note that both the PBD1 (**9**) and PBD2 (**10**) molecules studied by Raju and co-workers had large C8-substituents, and it is likely that they were

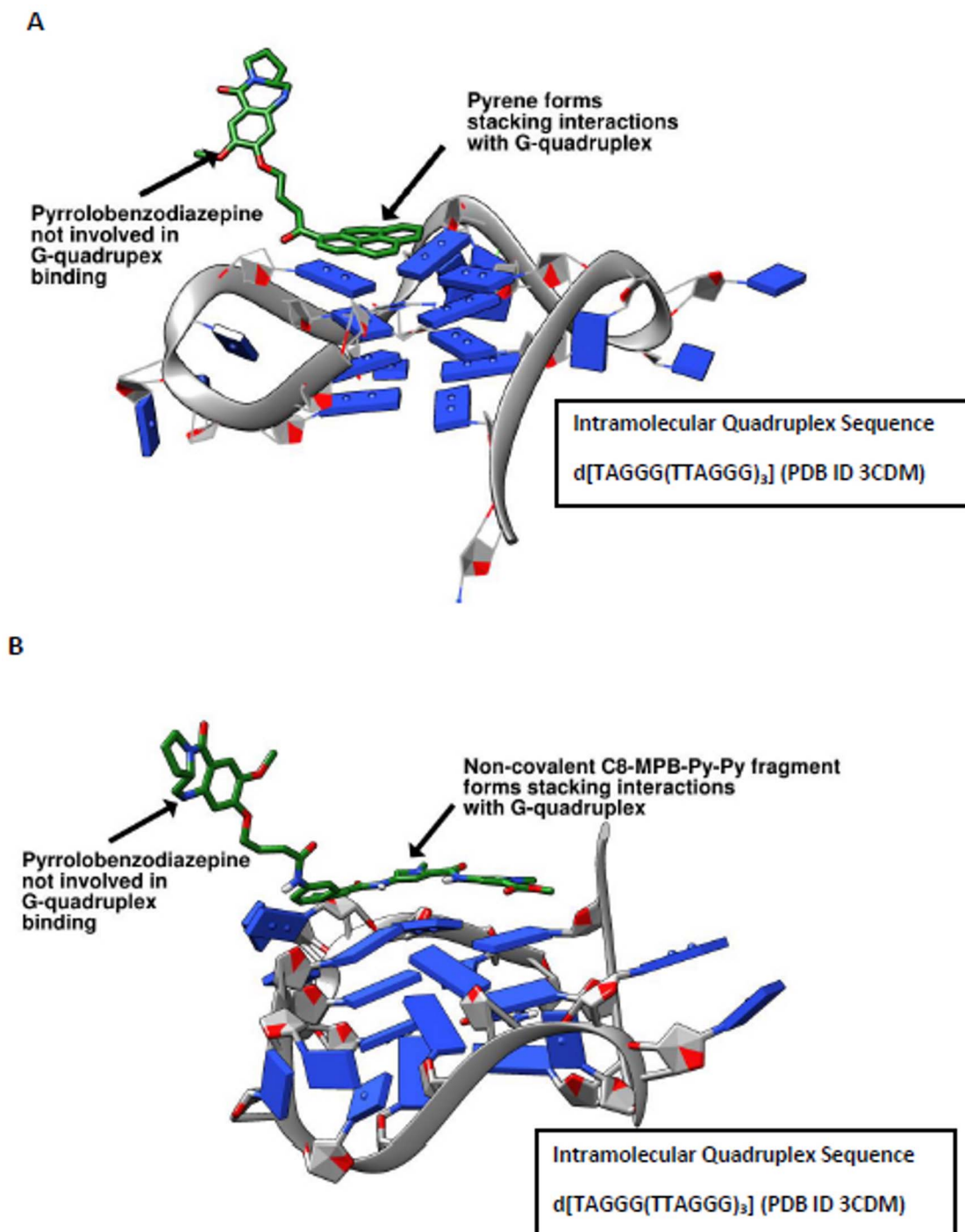


Figure 7. A, Snapshot of a MD simulation of the PBD-Pyrene conjugate (PBD1, **9**) interacting with the telomeric G-quadruplex, showing the the C8-pyrene component stacking with the G-quartet of the telomeric quadruplex, and the PBD component pointing upwards in an orthogonal orientation to the pyrene moiety; **B**, Snapshot of a MD simulation of the C8-PBD conjugate KMR-28-18 (**5**) interacting with the telomeric G-quadruplex, showing a similar interaction of the C8-side chain with the quadruplex DNA rather than the PBD moiety itself.
doi:10.1371/journal.pone.0105021.g007

observing the same non-specific interactions of the C8-substituents with the quadruplex DNA rather than the PBD moieties themselves.

We also note that, in their recent report in *this journal* [53], Raju and co-workers state that “PBDs were previously reported to possess planar structure and intercalate to DNA”, referring to work published by Hopkins and co-workers [70] and Kraus and

Selvakumar [71]. In fact, since the discovery of the first PBD (anthramycin) in the early 1960s [6], there have been no reports of this family of agents interacting with DNA by intercalation, and it is widely accepted that they are not planar due to their chiral C11a(S)-position and interact in the minor groove due to their inherent isohelicity with the DNA helix.

In summary, we report here experimental evidence that PBD molecules do not interact to any significant extent with quadruplex DNA structures. It is important that this is clear in the literature, as two PBD-based agents are presently in clinical trials and others are in late-stage pre-clinical development, and so the mechanism of action of these agents will be under close scrutiny in the future.

References

- Antonow D, Thurston DE (2011) Synthesis of DNA-interactive pyrrolo[2,1-c][1,4]benzodiazepines (PBDs). *Chem Rev* 111: 2815–2864.
- Cipolla L, Araujo AC, Airolodi C, Bini D (2009) Pyrrolo[2,1-c][1,4]benzodiazepine as a scaffold for the design and synthesis of anti-tumour drugs. *Anticancer Agents Med Chem* 9: 1–31.
- Gerrattana B (2012) Biosynthesis, synthesis, and biological activities of pyrrolobenzodiazepines. *Med Res Rev* 32: 254–293.
- Hartley JA (2011) The development of pyrrolobenzodiazepines as antitumour agents. *Expert Opin Investig Drugs* 20: 733–744.
- Kamal A, Reddy KL, Devaiah V, Shankaraiah N, Reddy DR (2006) Recent advances in the solid-phase combinatorial synthetic strategies for the benzodiazepine based privileged structures. *Mini Rev Med Chem* 6: 53–69.
- Leimgruber W, Stefanovic V, Schenker F, Karr A, Berger J (1965) Isolation and characterization of anthramycin, a new antitumor antibiotic. *J Am Chem Soc* 87: 5791–5793.
- Hurley LH, Reck T, Thurston DE, Langley DR, Holden KG, et al. (1988) Pyrrolo[1,4]benzodiazepine antitumor antibiotics: relationship of DNA alkylation and sequence specificity to the biological activity of natural and synthetic compounds. *Chem Res Toxicol* 1: 258–268.
- Rahman KM, James CH, Thurston DE (2011) Observation of the reversibility of a covalent pyrrolobenzodiazepine (PBD) DNA adduct by HPLC/MS and CD spectroscopy. *Organic & Biomolecular Chemistry* 9: 1632–1641.
- Kotecha M, Kluzaj J, Wells G, O'Hare CC, Forni C, et al. (2008) Inhibition of DNA binding of the NF-Y transcription factor by the pyrrolobenzodiazepine-polyamide conjugate GWL-78. *Mol Cancer Ther* 7: 1319–1328.
- Wells G, Howard PW, Martin C, Sands ZA, Loughton CA, et al. (2005) Design, synthesis, biophysical and biological evaluation of a series of methyl ester-terminated pyrrolobenzodiazepine (PBD)-poly(N-methylpyrrole) conjugates. *Clinical Cancer Research* 11: 9015s–9015s.
- Brucoli F, Hawkins RM, James CH, Jackson PJM, Wells G, et al. (2013) An Extended Pyrrolobenzodiazepine-Polyamide Conjugate with Selectivity for a DNA Sequence Containing the ICB2 Transcription Factor Binding Site. *J Med Chem* 56: 6339–6351.
- Rahman KM, Jackson PJM, James CH, Basu BP, Hartley JA, et al. (2013) GC-Targeted C8-Linked Pyrrolobenzodiazepine-Biaryl Conjugates with Femtomolar *In Vitro* Cytotoxicity and *In Vivo* Antitumor Activity in Mouse Models. *Journal of Medicinal Chemistry* 56: 2911–2935.
- Puvvada MS, Hartley JA, Jenkins TC, Thurston DE (1993) A quantitative assay to measure the relative DNA-binding affinity of pyrrolo[2,1-c][1,4]benzodiazepine (PBD) antitumor antibiotics based on the inhibition of restriction endonuclease BamHI. *Nucleic Acids Res* 21: 3671–3675.
- Clingen PH, De Silva IU, McHugh PJ, Ghadessy FJ, Tilby MJ, et al. (2005) The XPF-ERCC1 endonuclease and homologous recombination contribute to the repair of minor groove DNA interstrand crosslinks in mammalian cells produced by the pyrrolo[2,1-c][1,4]benzodiazepine dimer SJG-136. *Nucleic Acids Res* 33: 3283–3291.
- Puvvada MS, Forrow SA, Hartley JA, Stephenson P, Gibson I, et al. (1997) Inhibition of Bacteriophage T7 RNA Polymerase *In Vitro* Transcription by DNA-Binding Pyrrolo[2,1-c][1,4]benzodiazepines. *Biochemistry* 36: 2478–2484.
- Osada H, Uramoto M, Uzawa J, Kajikawa K, Isono K (1990) New Pyrrolobenzodiazepine antibiotics, RK-1441 A and B.2. Isolation and Structure. *Agricultural and Biological Chemistry* 54: 2883–2887.
- Hadjivassileva T, Thurston DE, Taylor PW (2005) Pyrrolobenzodiazepine dimers: novel sequence-selective, DNA-interactive, cross-linking agents with activity against Gram-positive bacteria. *Journal of Antimicrobial Chemotherapy* 56: 513–518.
- Fotso S (2010) Naturally Occurring Pyrrolo 1,4 benzodiazepines in Bacteria. *Mini-Reviews in Organic Chemistry* 7: 68–74.
- Fotso S, Zabriskie TM, Proteau PJ, Flatt PM, Santosa DA, et al. (2009) Limazepines A-F, Pyrrolo 1,4 benzodiazepine Antibiotics from an Indonesian *Micrococcus* sp. *Journal of Natural Products* 72: 690–695.
- Rahman KM, Rosado H, Moreira JB, Feuerbaum E-A, Fox KR, et al. (2012) Antistaphylococcal activity of DNA-interactive pyrrolobenzodiazepine (PBD) dimers and PBD-biaryl conjugates. *Journal of Antimicrobial Chemotherapy* 67: 1683–1696.
- Rosado H, Rahman KM, Feuerbaum E-A, Hinds J, Thurston DE, et al. (2011) The minor groove-binding agent ELB-21 forms multiple interstrand and intrastrand covalent cross-links with duplex DNA and displays potent

Acknowledgments

We are grateful to Spirogen Ltd (now part of AstraZeneca) for providing samples of GWL-78 (4), SJG-136 (6), DRG-16 (7) and ELB-21 (8).

Author Contributions

Conceived and designed the experiments: DET KMR. Performed the experiments: KMR PJMJ DC TTTB. Analyzed the data: DET KMR PJMJ. Wrote the paper: DET KMR PJMJ.

- bactericidal activity against methicillin-resistant *Staphylococcus aureus*. *Journal of Antimicrobial Chemotherapy* 66: 985–996.
- Barkley MD, Cheatham S, Thurston DE, Hurley LH (1986) Pyrrolo[1,4]benzodiazepine antitumor antibiotics: evidence for two forms of tomaymycin bound to DNA. *Biochemistry* 25: 3021–3031.
- Seifert J, Pezeshki S, Kamal A, Weisz K (2012) Inter- and Intrastrand DNA Crosslinks by 2-Fluoro-Substituted Pyrrolobenzodiazepine Dimers: Stability, Stereochemistry and Drug Orientation. *Organic & Biomolecular Chemistry* 10: 6850–6860.
- Smellie M, Bose DS, Thompson AS, Jenkins TC, Hartley JA, et al. (2003) Sequence-Selective Recognition of Duplex DNA Through Covalent Interstrand Cross-Linking: Kinetic and Molecular Modeling Studies With Pyrrolobenzodiazepine Dimers. *Biochemistry* 42: 8232–8239.
- Kopka ML, Goodsell DS, Baikalov I, Grzeskowiak K, Cascio D, et al. (1994) Crystal structure of a covalent DNA-drug adduct: anthramycin bound to C-C-A-A-C-G-T-T-G-G and a molecular explanation of specificity. *Biochemistry* 33: 13593–13610.
- Thurston DE (1993) Advances in the Study of Pyrrolo[2,1-c][1,4]benzodiazepine (PBD) Antitumor Antibiotics. In: Neidle S, Waring MJ, editors. *Molecular Aspects of Anticancer Drug-DNA Interactions*. London: The Macmillan Press Ltd., London, UK. pp. 54–88.
- Rahman KM, Vassoler H, James CH, Thurston DE (2010) DNA Sequence Preference and Adduct Orientation of Pyrrolo[2,1-c][1,4]benzodiazepine Antitumor Agents. *ACS Medicinal Chemistry Letters* 1: 427–432.
- Thurston DE (2006) *Chemistry and Pharmacology of Anticancer Drugs*. CRC Press (Taylor & Francis): Boca Raton, FL, 1: 281.
- Wells G, Martin CRH, Howard PW, Sands ZA, Loughton CA, et al. (2006) Design, synthesis, and biophysical and biological evaluation of a series of Pyrrolobenzodiazepine - Poly(N-methylpyrrole) conjugates. *Journal of Medicinal Chemistry* 49: 5442–5461.
- Rahman KM, Mussa V, Narayanaswamy M, James CH, Howard PW, et al. (2009) Observation of a dynamic equilibrium between DNA hairpin and duplex forms of covalent adducts of a minor groove binding agent. *Chemical Communications*: 227–229.
- Kamal A, Balakrishna G, Ramakrishna G, Shaik TB, Sreekanth K, et al. (2010) Synthesis and biological evaluation of cinnamido linked pyrrolo 2,1-c 1,4 benzodiazepines as antimitotic agents. *European Journal of Medicinal Chemistry* 45: 3870–3884.
- Kamal A, Devaiah V, Reddy KL, Kumar MS (2005) Synthesis and biological activity of fluoroquinolone-pyrrolo[2,1-c][1,4]benzodiazepine conjugates. *Bioorganic & Medicinal Chemistry* 13: 2021–2029.
- Kamal A, Khan MNA, Srikanth YVV, Reddy KS, Juvekar A, et al. (2008) Synthesis, DNA-binding ability and evaluation of antitumor activity of triazolo[1,2,4] benzothiadiazine linked pyrrolo[2,1-c][1,4] benzodiazepine conjugates. *Bioorganic & Medicinal Chemistry* 16: 7804–7810.
- Baraldi PG, Balboni G, Cacciari B, Guiotto A, Manfredini S, et al. (1999) Synthesis, *In Vitro* Antiproliferative Activity, and DNA-Binding Properties of Hybrid Molecules Containing Pyrrolo[2,1-c][1,4]benzodiazepine and Minor-Groove-Binding Oligopyrrole Carriers. *Journal of Medicinal Chemistry* 42: 5131–5141.
- Farmer JD, Rudnicki SM, Suggs JW (1988) Synthesis and DNA crosslinking ability of a dimeric anthramycin analog. *Tetrahedron Letters* 29: 5105–5108.
- Rahman KM, James CH, Thurston DE (2011) Effect of base sequence on the DNA cross-linking properties of pyrrolobenzodiazepine (PBD) dimers. *Nucleic Acids Research*.
- Rahman KM, Thompson AS, James CH, Narayanaswamy M, Thurston DE (2009) The Pyrrolobenzodiazepine Dimer SJG-136 Forms Sequence-Dependent Intrastrand DNA Cross-Links and Monoalkylated Adducts in Addition to Interstrand Cross-Links. *Journal of the American Chemical Society* 131: 13756–13766.
- Gregson SJ, Howard PW, Hartley JA, Brooks NA, Adams IJ, et al. (2001) Design, synthesis, and evaluation of a novel pyrrolobenzodiazepine DNA-interactive agent with highly efficient cross-linking ability and potent cytotoxicity. *J Med Chem* 44: 737–748.
- Hochhauser D, Meyer T, Spanswick VJ, Wu J, Clingen PH, et al. (2009) Phase I Study of Sequence-Selective Minor Groove DNA Binding Agent SJG-136 in Patients with Advanced Solid Tumors. *Clinical Cancer Research* 15: 2140–2147.

40. Janjigian YY, Lee W, Kris MG, Miller VA, Krug LM, et al. (2010) A Phase I Trial of SJG-136 (NSC#694501) in Advanced Solid Tumors. *Cancer Chemotherapy and Pharmacology* 65: 833–838.
41. Puzanov I, Lee W, Chen AP, Calcutt MW, Hachey DL, et al. (2011) Phase I Pharmacokinetic and Pharmacodynamic Study of SJG-136, a Novel DNA Sequence Selective Minor Groove Cross-linking Agent, in Advanced Solid Tumors. *Clinical Cancer Research* 17: 3794–3802.
42. Kamal A, Rajender, Reddy DR, Reddy MK, Balakishan G, et al. (2009) Remarkable enhancement in the DNA-binding ability of C2-fluoro substituted pyrrolo[2,1-*c*][1,4] benzodiazepines and their anticancer potential. *Bioorganic & Medicinal Chemistry* 17: 1557–1572.
43. Bates P, Mergny JL, Yang D (2007) Quartets in G-major - The first international meeting on quadruplex DNA. *Embo Reports* 8: 1003–1010.
44. Eddy J, Maizels N (2008) Conserved elements with potential to form polymorphic G-quadruplex structures in the first intron of human genes. pp. 1321–1333.
45. Campbell NH, Parkinson GN, Reszka AP, Neidle S (2008) Structural basis of DNA quadruplex recognition by an acridine drug. *Journal of the American Chemical Society* 130: 6722–+.
46. Burge S, Parkinson GN, Hazel P, Todd AK, Neidle S (2006) Quadruplex DNA: sequence, topology and structure. *Nucleic Acids Research* 34: 5402–5415.
47. Biffi G, Tannahill D, McCafferty J, Balasubramanian S (2013) Quantitative visualization of DNA G-quadruplex structures in human cells. *Nat Chem* 5: 182–186.
48. Lam EY, Beraldi D, Tannahill D, Balasubramanian S (2013) G-quadruplex structures are stable and detectable in human genomic DNA. *Nat Commun* 4: 1796.
49. Muller S, Kumari S, Rodriguez R, Balasubramanian S (2010) Small-molecule-mediated G-quadruplex isolation from human cells. *Nat Chem* 2: 1095–1098.
50. Balasubramanian S, Hurley LH, Neidle S (2011) Targeting G-quadruplexes in gene promoters: a novel anticancer strategy? *Nature Reviews: Drug Discovery* 10: 261–275.
51. Gomez D, Paterski R, Lemarteleur T, Shin-ya K, Mergny JL, et al. (2004) Interaction of telomestatin with the telomeric single-strand overhang. *Journal of Biological Chemistry* 279: 41487–41494.
52. Gabelica V, Baker ES, Teulade-Fichou MP, De Pauw E, Bowers MT (2007) Stabilization and structure of telomeric and c-myc region intramolecular G-quadruplexes: The role of central cations and small planar ligands. *Journal of the American Chemical Society* 129: 895–904.
53. Raju G, Srinivas R, Reddy VS, Idris MM, Kamal A, et al. (2012) Interaction of Pyrrolobenzodiazepine (PBD) Ligands with Parallel Intermolecular G-Quadruplex Complex Using Spectroscopy and ESI-MS. *Plos One* 7: e35920.
54. Kohn KW, Spears CL (1970) Reaction of Anthramycin with Deoxyribonucleic Acid. *Journal of Molecular Biology* 51: 551–572.
55. Rahman KR, Reszka AP, Gunaratnam M, Haider SM, Howard PW, et al. (2009) Biaryl Polyamides as a New Class of DNA Quadruplex-Binding Ligands. *Chemical Communications*: 4097–4099.
56. Rahman KM, Hossain MD, Sohrab MH, Drake AF, Bui TT, et al. (2012) The prenylated dioxopiperazine alkaloid Cristatin A has selective telomeric DNA G-quadruplex stabilising properties. *Chemical Communications* 48: 8760–8762.
57. Case D, Darden TA, Cheatham TE, Simmerling C, Wang J, et al. Amber 11.
58. Parkinson GN, Cuenca F, Neidle S (2008) Topology conservation and loop flexibility in quadruplex-drug recognition: crystal structures of inter- and intramolecular telomeric DNA quadruplex-drug complexes. *J Mol Biol* 381: 1145–1156.
59. Haider S, Neidle S (2010) Molecular Modeling and Simulation of G-Quadruplexes and Quadruplex-Ligand Complexes. In: Baumann P, editor. *G-Quadruplex DNA*: Humana Press. pp. 17–37.
60. Pérez A, Marchán I, Svozil D, Sponer J, Cheatham TE, et al. (2007) Refinement of the AMBER Force Field for Nucleic Acids: Improving the Description of alpha/gamma Conformers. *Biophysical journal* 92: 3817–3829.
61. Humphrey W, Dalke A, Schulten K (1996) VMD: visual molecular dynamics. *J Mol Graph* 14: 33–38, 27–38.
62. Pettersen EF, Goddard TD, Huang CC, Couch GS, Greenblatt DM, et al. (2004) UCSF Chimera—a visualization system for exploratory research and analysis. *J Comput Chem* 25: 1605–1612.
63. Fogolari F, Zuccato P, Esposito G, Viglino P (1999) Biomolecular electrostatics with the linearized Poisson-Boltzmann equation. *Biophys J* 76: 1–16.
64. Case DA, Darden TA, Cheatham III TE, Simmerling CL, Wang J, et al. (2010) AMBER 11, University of California, San Francisco, 2010.
65. Mergny JL, Maurizot JC (2001) Fluorescence resonance energy transfer as a probe for G-quartet formation by a telomeric repeat. *Chembiochem* 2: 124–132.
66. Darby RAJ, Sollogoub M, McKeen C, Brown L, Risitano A, et al. (2002) High throughput measurement of duplex, triplex and quadruplex melting curves using molecular beacons and a LightCycler. *Nucleic Acids Research* 30.
67. Parkinson GN, Ghosh R, Neidle S (2007) Structural basis for binding of porphyrin to human telomeres. *Biochemistry* 46: 2390–2397.
68. Yang D, Okamoto K (2010) Structural insights into G-quadruplexes: towards new anticancer drugs. *Future medicinal chemistry* 2: 619–646.
69. Ambrus A, Chen D, Dai J, Bialis T, Jones RA, et al. (2006) Human telomeric sequence forms a hybrid-type intramolecular G-quadruplex structure with mixed parallel/antiparallel strands in potassium solution. *Nucleic Acids Research* 34: 2723–2735.
70. Hopton SR, Thompson AS (2011) Nuclear Magnetic Resonance Solution Structures of Inter- and Intrastrand Adducts of DNA Cross-Linker SJG-136. *Biochemistry* 50: 4720–4732.
71. Kraus GA, Selvakumar N (1999) A novel Fremy's salt-mediated oxidation and rearrangement of anilines into amino ortho-diketones. Applications to the synthesis of pyrrolobenzodiazepines. *Tetrahedron Letters* 40: 2039–2040.